

E1-2012-13

Ts. Baatar¹, B. Batgerel^{1,2}, R. Togoo¹, A. I. Malakhov²,
B. Otgongerel¹, M. Sovd¹, B. Chadraa¹, N. G. Fadeev²,
G. Sharkhuu¹

A POSSIBLE STUDY OF THE PHASE TRANSITION
IN π^-C INTERACTION AT 40 GeV/c

Submitted to «Ядерная физика»

¹Institute of Physics and Technology, MAS, Ulaanbaatar, Mongolia

²Joint Institute for Nuclear Research, Dubna

Баатар Ц. и др.

E1-2012-13

Возможность изучения фазового перехода в π^-C -взаимодействии при 40 ГэВ/с

Рассмотрены импульсные и угловые характеристики протонов и π^- -мезонов, рожденных в π^-C -взаимодействиях при 40 ГэВ/с, как функция кумулятивного числа n_k (или четырехмерного переданного импульса t). Проведенный анализ указывает на возможное появление фазового перехода ядерной материи.

Работа выполнена в Лаборатории физики высоких энергий им. В. И. Векслера и А. М. Балдина ОИЯИ.

Препринт Объединенного института ядерных исследований. Дубна, 2012

Baatar Ts. et al.

E1-2012-13

A Possible Study of the Phase Transition in π^-C Interaction at 40 GeV/c

In this paper we consider the momentum and angular characteristics of protons and π^- mesons produced in π^-C interactions at 40 GeV/c as a function of the cumulative number n_k (or the four-dimensional momentum transfer t). Analysis carried out in this paper indicates possible appearance of the phase transition of nuclear matter.

The investigation has been performed at the Veksler and Baldin Laboratory of High Energy Physics, JINR.

Preprint of the Joint Institute for Nuclear Research. Dubna, 2012

1. INTRODUCTION

The investigation of the multiparticle production process in hadron–nucleus and nucleus–nucleus interactions at high energies and large momentum transfers is very important for understanding the strong interaction mechanism and inner quark–gluon structure of nuclear matter.

During the last years, the possibility of observing the collective phenomena such as the cumulative particle production [1], the production of nuclear matter with high densities, the phase transition from the hadronic matter to the quark–gluon plasma state is widely discussed in the literature [2–5, 11, 12].

According to different ideas and models, if these phenomena exist in the nature, then they will be observed in the hadron–nucleus and nucleus–nucleus interactions at high energies and large momentum transfers and should be influenced by the dynamics of interaction process and would be reflected in the angular and momentum characteristics of the reaction products.

In hadron–nucleus and nucleus–nucleus interactions, in contrast to hadron–nucleon interactions, the secondary particles may be produced as a result of multinucleon interactions, in other words, the particles are produced in the region kinematically forbidden for hadron–nucleon interactions. This fact is one of the reasons of interest for studying the nucleus collision at high energies.

In this paper we are considered the next reactions:

$$\pi^- C \longrightarrow p + X, \quad (1)$$

$$\pi^- C \longrightarrow \pi^- + X. \quad (2)$$

This paper is a continuation of our previous publications [6, 7].

2. VARIABLES USED

2.1. Cumulative Number. The cumulative number n_k in the fixed target experiment is determined by the next formula

$$n_k = \frac{P_a \cdot P_c}{P_a \cdot P_b} \simeq \frac{E_c - P_{\parallel}^c}{m_p}. \quad (3)$$

Here P_a , P_b , and P_c are the four-dimensional momenta of the incident particle, target, and the considered secondary particles, correspondingly; E_c is the energy, and P_{\parallel}^c is the longitudinal momentum of the considered particle, m_p is the proton mass. From this formula we see that this variable is **relativistic invariant**.

This variable (n_k) may be interpreted as a minimal target mass, which is required for producing the given secondary particle, because at summarizing by all secondary particles, there should be obtained the value of the target mass determined on the basis of the energy–momentum conservation law, i.e.,

$$M_t \simeq \frac{\sum_{i=1}^n (E - P_{\parallel})_i}{m_p}. \quad (4)$$

So, n_k distribution gives the **ordered mass values** from the target required for producing the considered secondary particles.

The connection between the variable n_k and momentum transfer t is determined by the next formula [7]:

$$t = -Q^2 = -m_{\pi}^2 - m_c^2 + S_{\pi-p} \cdot n_k \approx S_{\pi-p} \cdot n_k, \quad (5)$$

where $S_{\pi-p}$ is the total energy square of π^-p interaction. In this experiment, $S_{\pi-p} \cong 2E_a \cdot m_p \cong 75 \text{ GeV}^2/c^2$ is constant. To study the phase transition of the nuclear matter we must choose the variables corresponding to this physical process. In the theoretical calculations, the effective temperature T , the density of nuclear matter ρ/ρ_0 or the chemical potential μ are mainly used. But the variables μ and ρ are not fully determined experimentally. So for studying the phase transition process we must select the other appropriate variable. With this goal let us consider formula (5) which gives the connection between the variables n_k and t . From this formula one can see that with increasing t the minimal mass value n_k , which is required from the target for producing the considered secondary particle, increases or vice versa. This means that if any one particle with $n_k > 1$ (cumulative particle) is produced in hadron–nucleus interactions at high energies, then this particle should be produced at large momentum transfers more than the total energy square of π^-p interaction $S_{\pi-p}$, i.e., $t > S_{\pi-p}$, for example, if $n_k = 1.5$, then only for this particle $t \cong S_{\pi-p} \cdot n_k = 75 \text{ GeV}^2/c^2 \cdot 1.5 = 112.5 \text{ GeV}^2/c^2$ which is not allowed for π^-p interactions.

On the other hand, if two particles are produced at two different values of n_k ($Q_1^2 < Q_2^2$), then the size of the particle-production region for every particle is different and may be estimated by the formulae $r_1 \sim 1/Q_1$, $r_2 \sim 1/Q_2$ and satisfies the condition $r_1 > r_2$, i.e. the size of the particle-emission region at high Q^2 is smaller than in the case at low Q^2 .

As a result of these two features (increasing of the mass ($n_k \cdot m_p$) and decreasing of the distance r) of the variable n_k (or t), the density of the nuclear matter ρ increases with increasing of n_k . In this sence, n_k (or t) is the more

appropriate variable to study the phase transition process of nuclear matter. In this case, the density of nuclear matter ρ may be determined by the next formula:

$$\rho = \frac{m}{V} = \frac{n_k \cdot m_p}{V}, \quad (6)$$

where V is the volume from which the particle is emitted. The volume V may be estimated as a sphere, i.e.,

$$V = \frac{4\pi}{3}r^3. \quad (7)$$

2.2. The Effective Temperature T . The transverse energy spectra of the secondary particles in the different n_k intervals are approximated by exponential functions of the next form:

$$\frac{1}{2 \cdot E_t} \frac{\Delta N}{\Delta E_t} \sim e^{-b \cdot E_t}, \quad E_t = \sqrt{p_t^2 + m^2}. \quad (8)$$

The effective temperature T is determined as the inverse of the slope parameters b ,

$$T = \frac{1}{b}. \quad (9)$$

3. EXPERIMENTAL METHOD

The experimental material was obtained with the help of Dubna 2-meter propane (C_3H_8) bubble chamber exposed to π^- mesons with momentum 40 GeV/c from Serpukhov accelerator. According to the advantage of the bubble chamber experiment, all distributions in this paper are obtained in the condition of 4π geometry of secondary particles.

The average error of the momentum measurements is $\sim 12\%$, and the average error of the angular measurements is $\sim 0.6^\circ$.

All secondary negative particles are taken as π^- mesons. The average boundary momentum from which π^- mesons were well identified in the propane bubble chamber is ~ 70 MeV/c. In connection with the identification problem between energetic protons and π^+ mesons, protons with momentum more than ~ 1 GeV/c are included into π^+ mesons.

The other experimental details are described in [8, 9].

4. STATISTICS

8791 π^-C interactions are used in this analysis.

1. The total number of protons is 12441.
2. The total number of π^- -mesons is 30145.

5. $\pi^- + C \rightarrow p + X$ ANALYSIS

It is interesting to stress that in this experiment the incident particles are π^- mesons. This means that the secondary protons in $\pi^- C$ interactions at 40 GeV/c should be produced only in the target fragmentation region, in other words, there is no overlapping from the projectile fragmentation region in the rapidity distribution of protons.

Figure 1 shows the n_k distribution of the secondary protons produced in $\pi^- C$ interactions at 40 GeV/c. From this distribution we see that many protons are produced in the region with $n_k > 1$ (cumulative protons). This distribution continues until $n_k \approx 2.3$.

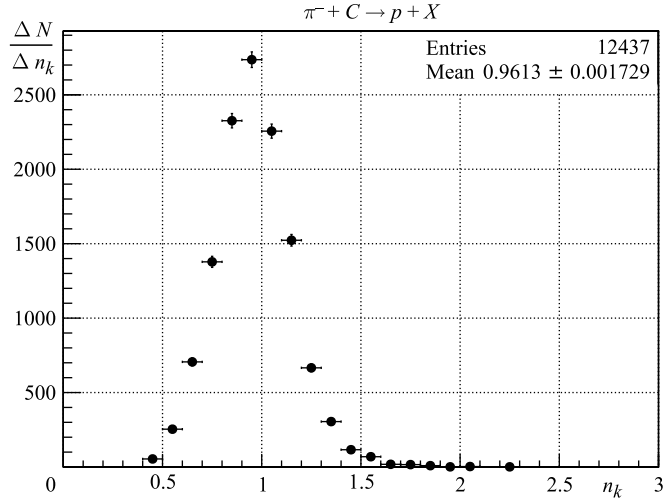


Fig. 1. Cumulative number (n_k) distribution of protons

Figure 2 gives the rapidity (y_{lab}) distribution of protons. This distribution shows the protons from $\pi^- C$ interactions are produced in the target fragmentation region.

Figure 3 presents the dependence of the average momentum of protons as a function of variable n_k . We see that with increasing n_k the average values of the momentum $\langle P_{total} \rangle$ are decreasing and reach the minimum at $n_k \approx 1$ and then in the region of cumulative particle production ($n_k > 1$) are increasing.

Figure 4 shows the dependence of the average values of the square of the transverse momentum as a function of the variable n_k . $\langle p_T^2 \rangle$ of protons on the variable n_k in the beginning are slowly growing until $n_k \approx 1.2$ and then we observe the essential increasing.

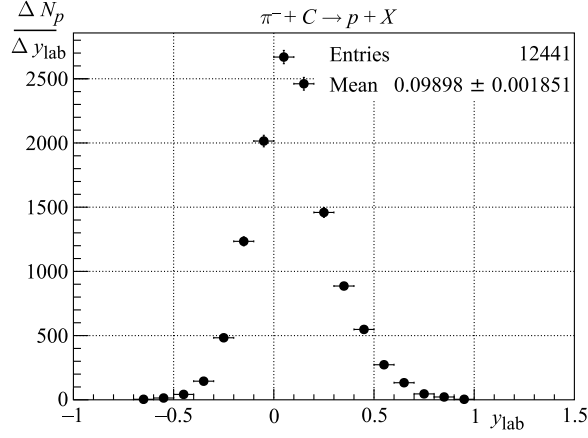


Fig. 2. Rapidity distribution of protons

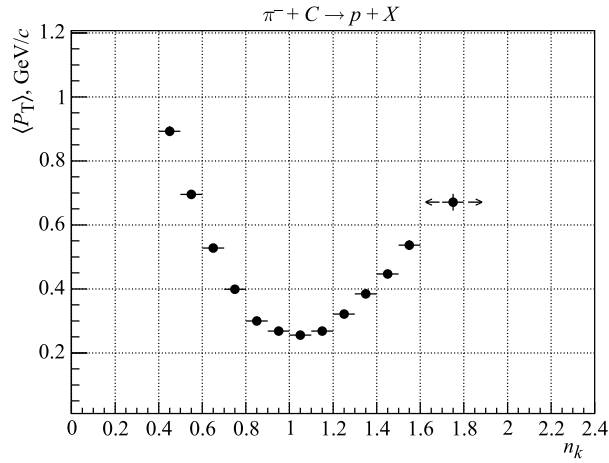


Fig. 3. The average values of the momentum of the secondary protons as a function of the variable n_k

Figure 5 shows the dependence of the average values of the emission angles of protons $\langle \Theta \rangle$ as a function of the variable n_k . We see that $\langle \Theta \rangle$ essentially increase until $n_k \simeq 1.2-1.3$ and then remain practically constant on the level $\langle \Theta \rangle \simeq 145^\circ$.

The transverse energy (or transverse momentum) spectrum of the secondary particles produced in hA and AA interactions at high energies may reflect the dynamics of the interaction process more clearly. This is connected with the fact that the transverse effects are mainly generated during the interaction process.

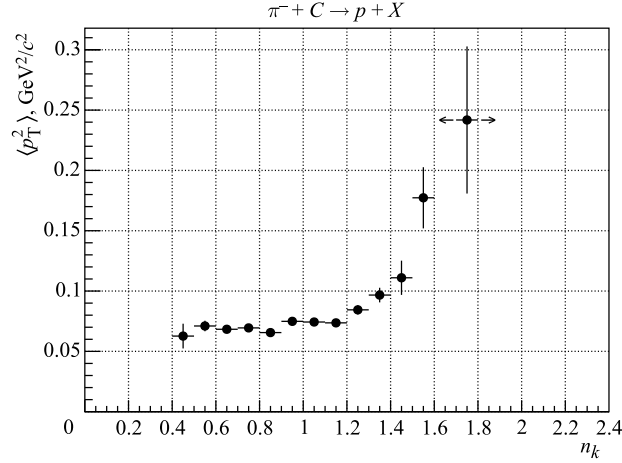


Fig. 4. The average values of the transverse momentum square as a function of the variable n_k

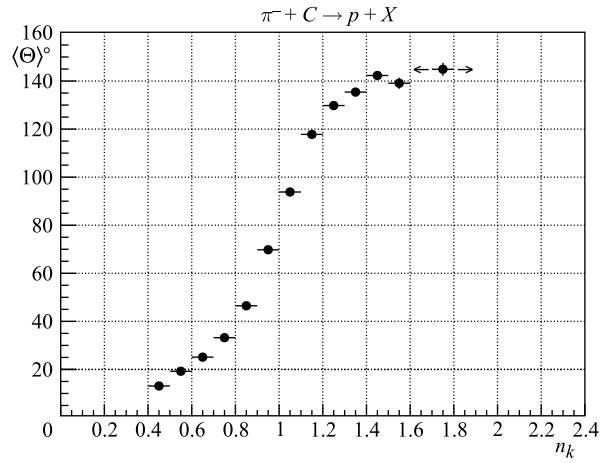


Fig. 5. The average values of the emission angles of protons as a function of the variable n_k

In connection with this in Fig. 6 are shown the transverse energy (E_t) spectrum of protons in different n_k intervals.

The experimental spectrum obtained in the every n_k interval is approximated by the exponential function (8), and the values of the slope parameters b and the effective temperatures T on the variable n_k are shown in Fig. 7. Figures 6, *a, b*, 7 and Table 1 show that the effective temperatures T remained

practically constant on the level $T \simeq 50$ MeV until $n_k \simeq 1.2-1.3$ and then essentially increase. T may be expressed by Kelvin temperature, then $T_{\text{plateau}}^p = 50 \text{ MeV} = 0.58 \cdot 10^{12} \text{ K}$, $T_{\text{max}}^p = 131 \text{ MeV} = 1.52 \cdot 10^{12} \text{ K}$ where T_{plateau}^p

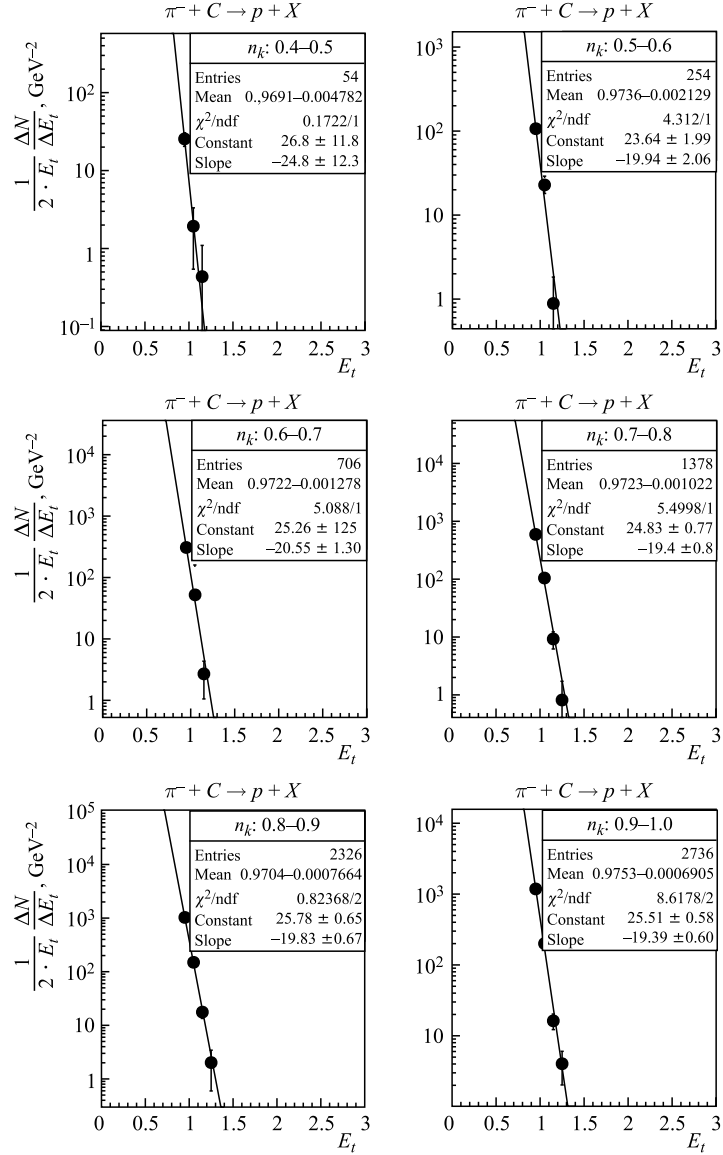


Fig. 6, a. Transverse energy E_t spectrum of protons as a function of different n_k intervals

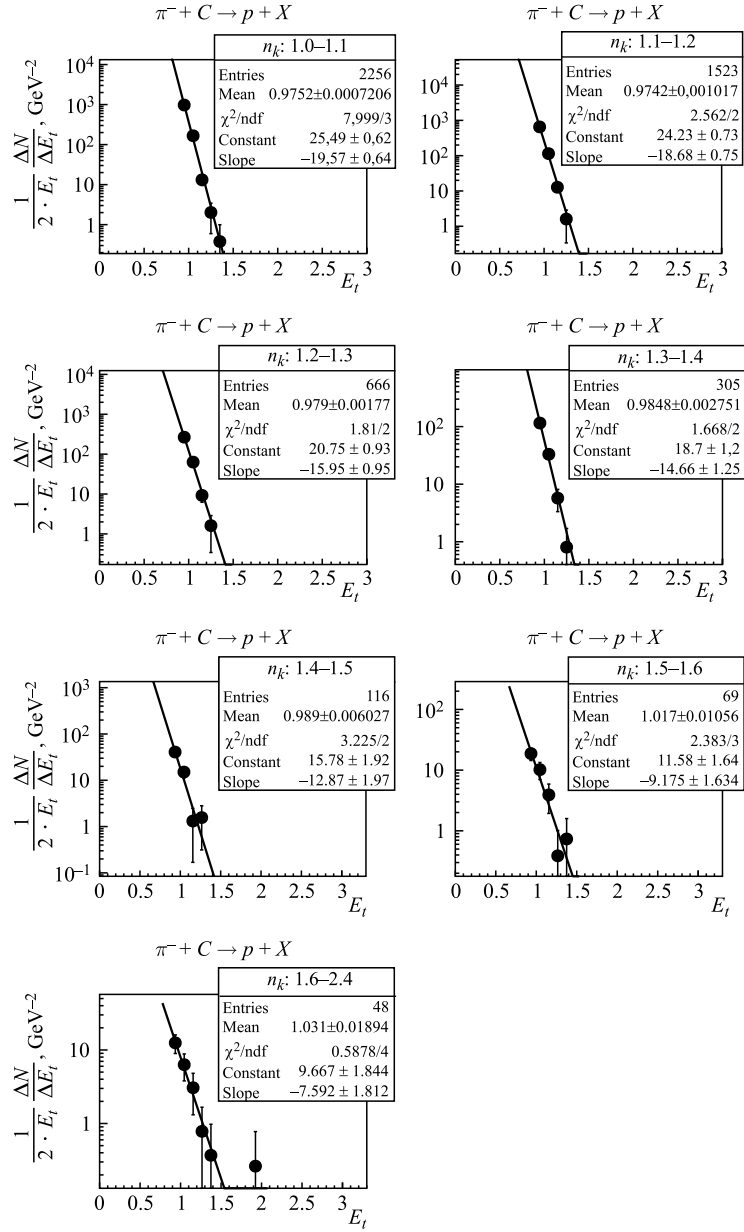


Fig. 6, *b*. Transverse energy E_t spectrum of protons as a function of different n_k intervals

Table 1. The values of the slope parameter b and the effective temperatures T on the variable n_k of protons from $\pi^- C$ interactions

Δn_k	b	T , GeV
0.4 ÷ 0.5	-24.8 ± 12.3	0.040 ± 0.019
0.5 ÷ 0.6	-19.94 ± 2.06	0.050 ± 0.005
0.6 ÷ 0.7	-20.55 ± 1.30	0.048 ± 0.003
0.7 ÷ 0.8	-19.4 ± 0.8	0.052 ± 0.002
0.8 ÷ 0.9	-19.83 ± 0.67	0.050 ± 0.001
0.9 ÷ 1.0	-19.39 ± 0.60	0.051 ± 0.001
1.0 ÷ 1.1	-19.57 ± 0.64	0.051 ± 0.001
1.1 ÷ 1.2	-18.68 ± 0.75	0.053 ± 0.002
1.2 ÷ 1.3	-15.95 ± 0.95	0.062 ± 0.003
1.3 ÷ 1.4	-14.66 ± 1.25	0.068 ± 0.005
1.4 ÷ 1.5	-12.87 ± 1.97	0.077 ± 0.011
1.5 ÷ 1.6	-9.17 ± 1.16	0.108 ± 0.019
1.6 ÷ 2.4	-7.59 ± 1.80	0.131 ± 0.031

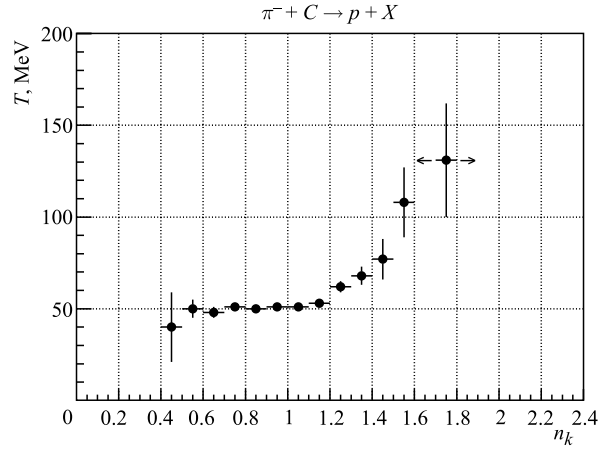


Fig. 7. The effective temperature T of the secondary protons as a function of the variable n_k

and T_{\max}^p are the effective temperatures corresponding to region $n_k^p \leq 1.2$ and $n_k^p = 1.75m_p$. For QGP state QCD predicts $T \simeq 2 \cdot 10^{12} K$. Now if we suppose the particle is emitted from the spherical volume V which is determined by formula (7), then we can give the estimation of the density of the nuclear matter in the hA interactions at high energies using formula (6); $\rho_{n_k=1.2}^p \longrightarrow$

$\frac{1.2m_p}{V} = \frac{1.2m_p}{0.082fm^3} = 14.6m_p/fm^3$, $\rho_{n_k=1.75}^p \longrightarrow \frac{1.75m_p}{V} = \frac{1.75m_p}{0.039fm^3} = 44.9m_p/fm^3$. Where $\rho_{n_k=1.2}^p$ and $\rho_{n_k=1.75}^p$ are the estimations of the densities corresponding to the regions $n_k = 1.2$ and $n_k = 1.75$.

6. $\pi^- + C \longrightarrow \pi^- + X$ ANALYSIS

As in the case of protons, the angular and momentum characteristics of π^- mesons from π^-C interaction at 40 GeV/c as a function of the variable n_k are carried out here.

Figure 8 presents the cumulative number (n_k) distribution of π^- mesons from π^-C interactions at 40 GeV/c. This distribution shows n_k distribution for π^- mesons continues until $n_k \simeq 5$.

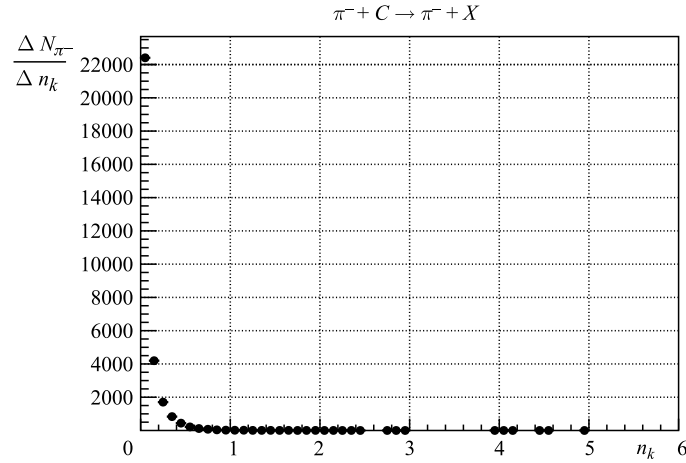


Fig. 8. The cumulative number (n_k) distribution of π^- mesons from π^-C interactions

The rapidity distribution of all π^- mesons from π^-C interactions is shown in Fig. 9.

Figure 10 shows the dependence of the average values of the momentum $\langle P_{total} \rangle$ of the secondary π^- -mesons as a function of the variable n_k . This distribution shows that $\langle P_{total} \rangle$ of π^- -mesons, as in the case of protons, decreased and reach the minimum value at $n_k \simeq 0.4-0.5$ and then they increased. We would like to note that in both cases of protons and π^- mesons, the characters of dependences of $\langle P_{total} \rangle$ on n_k are similar, but with different values of n_k which gives the minimum of these dependences.

Figure 11 presents the dependence of the average values of the transverse momentum square of π^- mesons on the variable n_k . From this figure we see

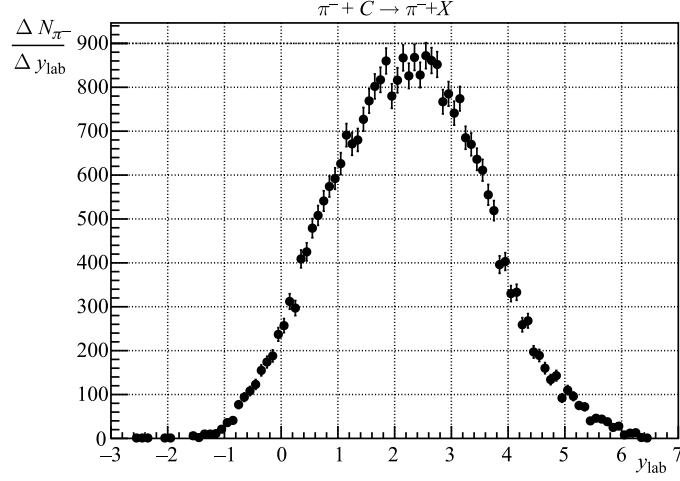


Fig. 9. The rapidity distribution of π^- mesons

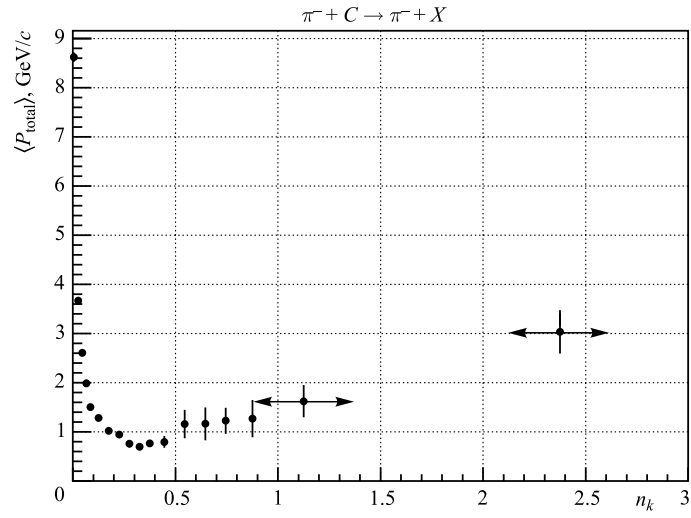


Fig. 10. The average value of the momentum of the secondary π^- mesons as a function of the variable n_k

that $\langle p_T^2 \rangle$ of π^- mesons slowly increase until $n_k \simeq 0.5$ and then the dependence becomes more strong.

Figure 12 shows the dependence of the average values of the angular distributions $\langle \theta \rangle$ of π^- mesons on the variable n_k . With increasing n_k , $\langle \theta \rangle$ increases

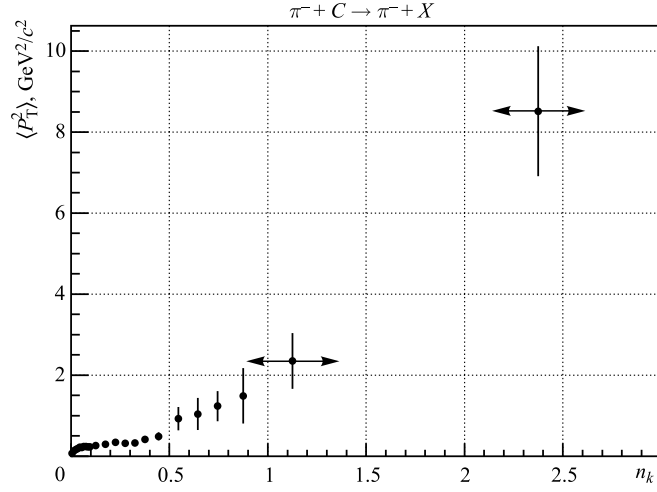


Fig. 11. The average value of the transverse momentum square of π^- -mesons on the variable n_k

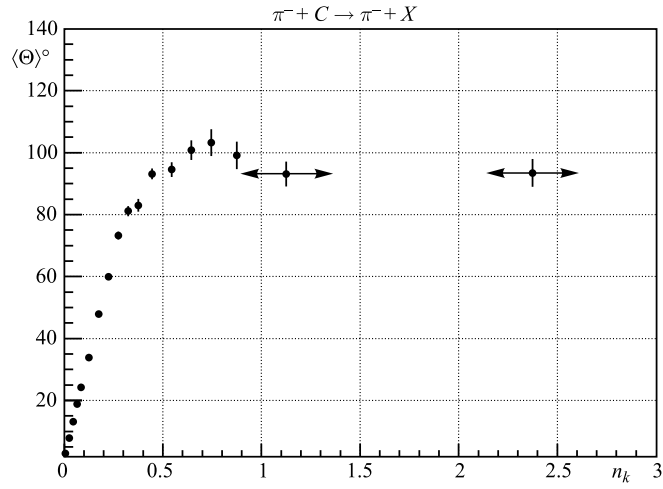


Fig. 12. The average value of the angular distribution of π^- mesons on the variable n_k

and beginning from the $n_k \simeq 0.5-0.6$ goes to the plateau on the level $\langle \theta \rangle_{\pi^-} \simeq 95^\circ$. We would like to note that the average values of the emission angles go to plateaus for protons ($\langle \theta \rangle_p \simeq 145^\circ$) and π^- mesons ($\langle \theta \rangle_{\pi^-} \simeq 95^\circ$) as a function of n_k and they are essentially different.

Figure 13, *a, b, c* shows the transverse energy (E_t) spectrum of π^- mesons as a function of different n_k intervals. The spectrum in the every n_k interval is well approximated by the exponential function (8), and the slope parameter b and the effective temperature T are given in Table 2.

Table 2. **The values of the slope parameter b and the effective temperature T on the variable n_k of π^- mesons from π^-C interactions**

Δn_k	b	T , GeV
0.0 ÷ 0.01	-10.3 ± 0.1	0.097 ± 0.008
0.01 ÷ 0.02	-7.38 ± 0.11	0.135 ± 0.002
0.02 ÷ 0.03	-6.343 ± 0.104	0.157 ± 0.002
0.03 ÷ 0.04	-6.05 ± 0.12	0.165 ± 0.003
0.04 ÷ 0.05	-5.867 ± 0.143	0.176 ± 0.005
0.05 ÷ 0.06	-5.718 ± 0.190	0.181 ± 0.006
0.06 ÷ 0.07	-5.584 ± 0.217	0.199 ± 0.012
0.07 ÷ 0.08	-4.656 ± 0.235	0.240 ± 0.005
0.08 ÷ 0.09	-4.325 ± 0.143	0.231 ± 0.007
0.09 ÷ 0.10	-4.317 ± 0.143	0.231 ± 0.007
0.1 ÷ 0.15	-4.361 ± 0.139	0.229 ± 0.007
0.15 ÷ 0.2	-4.232 ± 0.172	0.236 ± 0.009
0.2 ÷ 0.25	-4.216 ± 0.216	0.237 ± 0.012
0.25 ÷ 0.3	-4.39 ± 0.28	0.227 ± 0.014
0.3 ÷ 0.35	-4.289 ± 0.313	0.233 ± 0.017
0.35 ÷ 0.4	-3.811 ± 0.316	0.262 ± 0.021
0.4 ÷ 0.5	-3.88 ± 0.34	0.257 ± 0.022
0.5 ÷ 0.6	-3.632 ± 0.459	0.275 ± 0.034
0.6 ÷ 0.7	-3.464 ± 0.491	0.288 ± 0.040
0.7 ÷ 0.8	-3.151 ± 0.471	0.317 ± 0.47
0.8 ÷ 1.0	-2.196 ± 0.392	0.455 ± 0.081
1.0 ÷ 1.5	-1.486 ± 0.334	0.672 ± 0.151
1.5 ÷ 5.0	-0.7793 ± 0.2005	1.283 ± 0.330

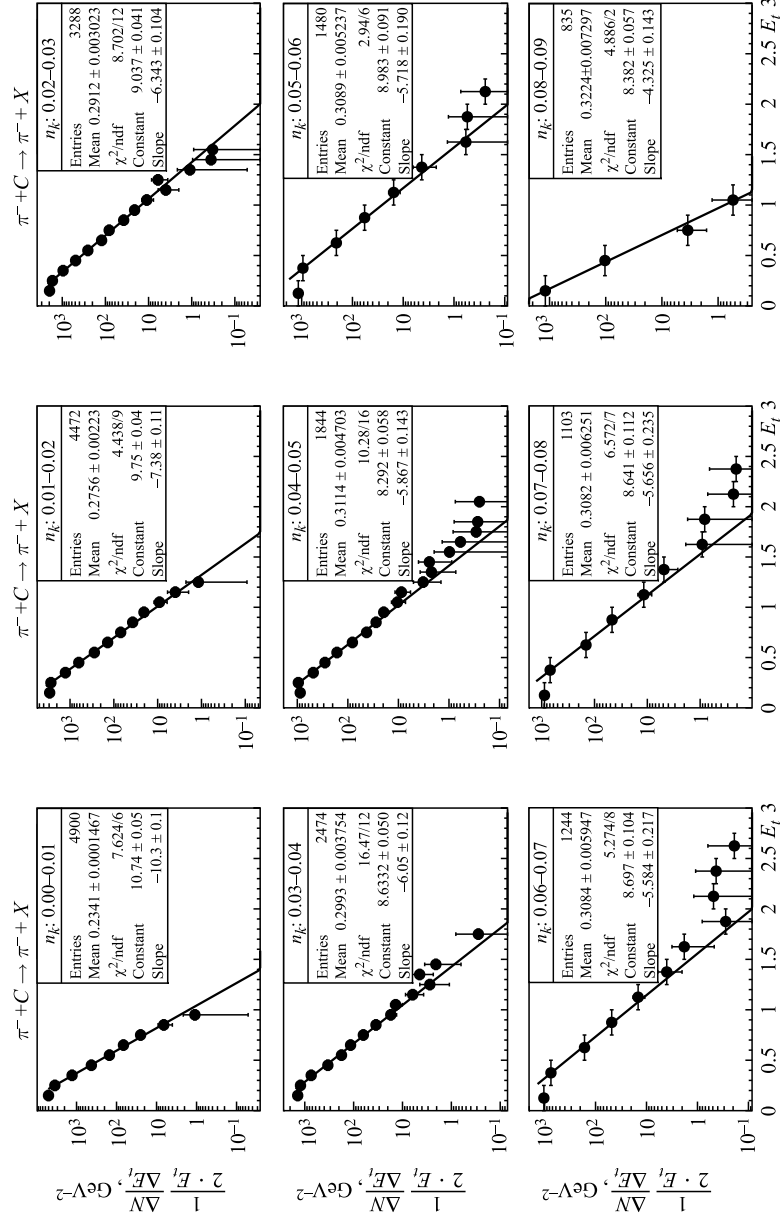


Fig. 13. a. Transverse energy E_t spectrum of π^- mesons as a function of different n_k intervals

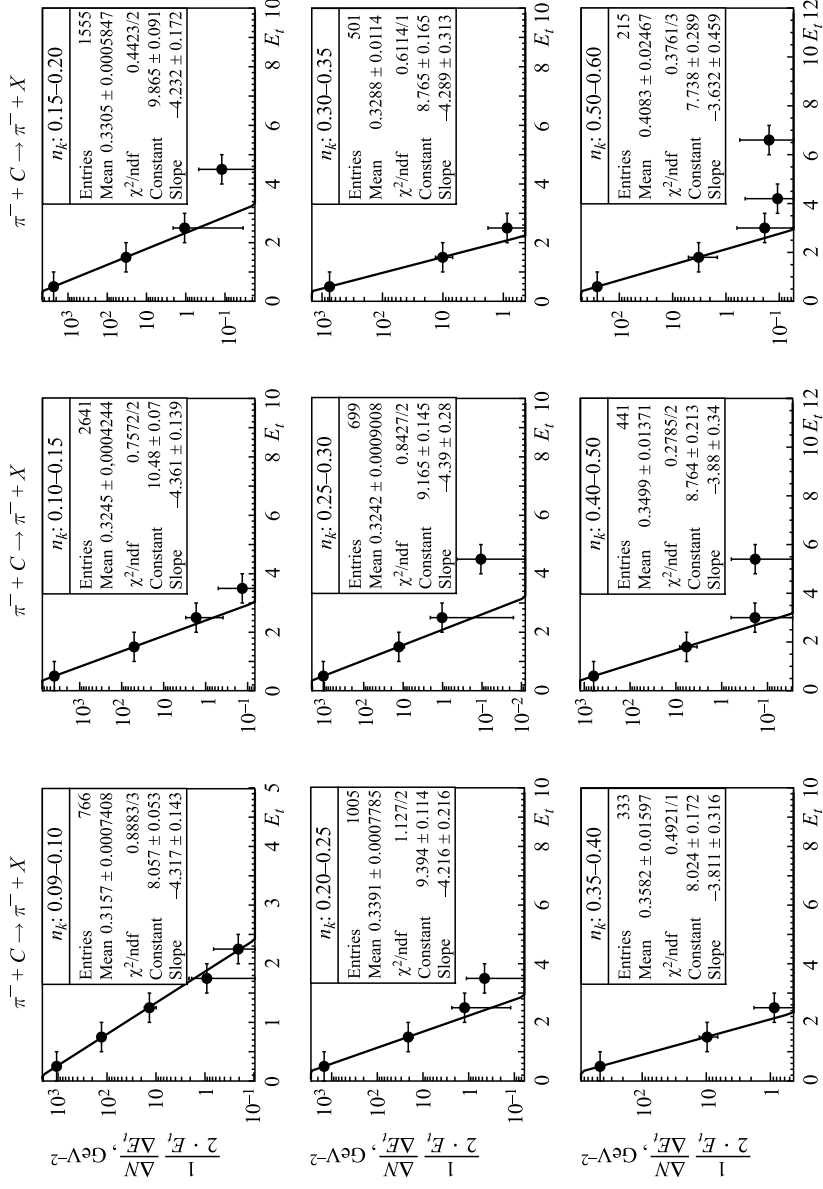


Fig. 13. *b*. Transverse energy E_t spectrum of π^- mesons as a function of different n_k intervals

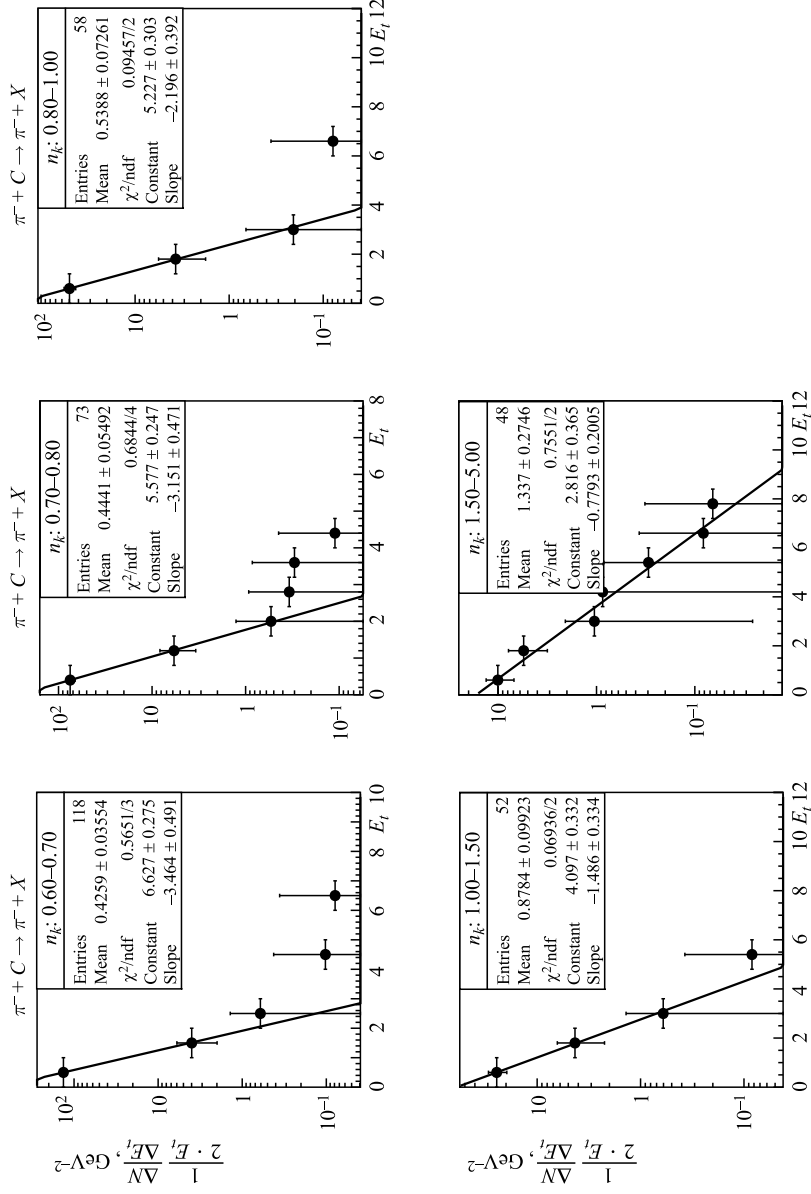


Fig. 13, c. Transverse energy E_t spectrum of π^- mesons as a function of different n_k intervals

The dependence of T parameters for π^- mesons from π^-C interactions as a function of n_k is shown in Fig. 14. From this figure we see that with increasing n_k , the effective temperatures T in the beginning are increasing until $n_k \simeq 0.1$, and then in the $n_k \simeq 0.1-0.5$ interval the parameter T remains practically constant on the level $T \simeq 0.220-0.230$ GeV and then it essentially increases.

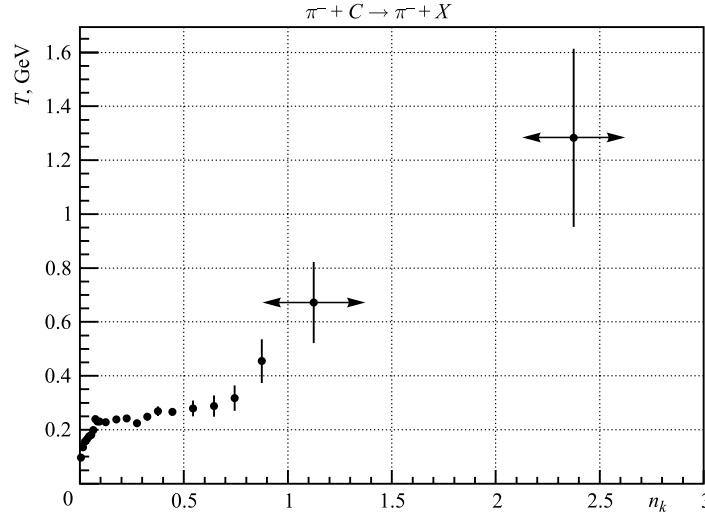


Fig. 14. The effective temperature T of the secondary π^- mesons as a function of the variable n_k

7. AVERAGE MULTIPLICITIES OF THE K_s^0 AND Λ^0 PARTICLES ON THE VARIABLE n_k

Using the data with the measured K_s^0 and Λ^0 particles in π^-C interactions at 40 GeV/c, we determined the $\langle N_{K^0} \rangle$ and $\langle N_{\Lambda^0} \rangle$ in the two different regions of the variable n_k .

This data consists of 5586 π^-C interactions and in these interactions we detected and measured 554 K^0 mesons and 331 Λ^0 hyperons after all corrections [10], and used the average weights: $\bar{w}_{K^0} = 3.4$ and $\bar{w}_{\Lambda^0} = 1.89$.

Average multiplicities of K^0 mesons and Λ^0 hyperons are taken from [10].

$$\langle N_{K^0} \rangle = 0.33 \pm 0.03, \quad (10)$$

$$\langle N_{\Lambda^0} \rangle = 0.11 \pm 0.02. \quad (11)$$

In this paper we determined $\langle N_{K^0} \rangle$ and $\langle N_{\Lambda^0} \rangle$ in two different regions of n_k . The first region is taken for protons $n_k < 1.2$ and for π^- mesons $n_k < 0.6$

and the second region — for protons $n_k \geq 1.2$ and for π^- mesons $n_k \geq 0.6$, and so on. Numbers of events, average multiplicities of K^0 mesons and Λ^0 hyperons are presented in Table 3, and we see that $\langle N_{K^0} \rangle$ and $\langle N_{\Lambda^0} \rangle$ practically remain constant in the first region of n_k and in the second region they essentially increase.

Table 3. **Average multiplicities of K^0 mesons and Λ^0 hyperons in different n_k regions**

	N_{event}	$\langle K^0 \rangle$	$\langle \Lambda^0 \rangle$
$n_k^p > 1.2; n_k^{\pi^-} > 0.6$	849	0.372 ± 0.050	0.121 ± 0.017
$n_k^p < 1.2; n_k^{\pi^-} < 0.6$	4737	0.330 ± 0.018	0.111 ± 0.007
$n_k^p > 1.3; n_k^{\pi^-} > 0.7$	428	0.432 ± 0.075	0.113 ± 0.024
$n_k^p < 1.3; n_k^{\pi^-} < 0.7$	5158	0.328 ± 0.018	0.112 ± 0.007
$n_k^p > 1.4; n_k^{\pi^-} > 0.8$	202	0.648 ± 0.140	0.145 ± 0.043
$n_k^p < 1.4; n_k^{\pi^-} > 0.8$	5384	0.325 ± 0.017	0.111 ± 0.007
$n_k^p > 1.5; n_k^{\pi^-} > 0.9$	118	0.809 ± 0.199	0.188 ± 0.068
$n_k^p < 1.5; n_k^{\pi^-} < 0.9$	5468	0.326 ± 0.017	0.111 ± 0.007
$n_k^p > 1.6; n_k^{\pi^-} > 1.0$	68	1.063 ± 0.325	0.234 ± 0.112
$n_k^p < 1.6; n_k^{\pi^-} < 1.0$	5518	0.327 ± 0.017	0.111 ± 0.007

8. DISCUSSION

In this paper we considered the dependences of the angular and momentum characteristics of the secondary protons and π^- mesons produced in π^-C interactions at 40 GeV/c as a function of the variable n_k . Average values of the momentum $\langle P_{\text{total}} \rangle$, average values of the square of the transverse momentum $\langle p_T^2 \rangle$, average multiplicities of the neutral strange particles $\langle N_{K^0} \rangle$, $\langle N_{\Lambda^0} \rangle$, and the effective temperature T on the variable n_k for protons show that every dependence consists of two parts: in the first part with $n_k < 1.2$, $\langle P_{\text{total}} \rangle_p$ decreases in the beginning and reaches the minimum at $n_k \simeq 1.0$ (Fig. 3), $\langle p_T^2 \rangle_p$ slowly increases until $n_k \simeq 1.2$ (Fig. 4), $\langle N_{K^0} \rangle$, $\langle N_{\Lambda^0} \rangle$ (Table 3), and the effective temperature T (Fig. 7) remains practically constant; in the second part with $n_k \geq 1.2$, $\langle P_{\text{total}} \rangle_p$, $\langle p_T^2 \rangle_p$, $\langle N_{K^0} \rangle$, $\langle N_{\Lambda^0} \rangle$, and T , contrary to the first part, essentially increase.

Now we consider the π^- meson case. In this experiment, the secondary π^- mesons are produced in the projectile fragmentation, central, and target fragmentation regions (Fig. 9).

With the increasing variable n_k , $\langle P_{\text{total}} \rangle_{\pi^-}$ decrease and reach the minimum at $n_k \simeq 0.4-0.5$ and then they are essentially increasing (Fig. 10) as in the case of protons. We would like to note that the n_k values which give the minima for protons ($n_k \simeq 1.0$) and for π^- mesons ($n_k \simeq 0.4$) are different. $\langle p_T^2 \rangle_{\pi^-}$ and the parameters T for π^- mesons contrary to the proton case, are noticeably increasing until $n_k \simeq 0.1$ and then the dependences remain practically constant (or increase very slowly) until $n_k \simeq 0.4 \div 0.5$ and then in the region $n_k \geq 0.5$ they again give the essential increasing. So we observe the essential changing of the behaviours of the angular and momentum characteristics of protons and π^- mesons from π^-C interactions at 40 GeV/c on the variable n_k in two different regions for protons and in three different regions for π^- mesons. Such behaviours may suggest different mechanism of particle production in these regions of the variable n_k (or t) and temperature T . If so, the first region with $n_k < 0.1$ $T \leq 0.220$ GeV for π^- mesons is connected with the thermalization of the strongly interacting objects, and the second region with $0.1 < n_k \leq 0.5$ for π^- mesons and $0.4 < n_k \leq 1.2$ for protons in which the parameter T is practically constant, may suggest that the equilibrium state formation (hadron+QGP state) and the third region with $n_k \geq 0.5$ for mesons and $n_k \geq 1.2$ for protons can be connected with the production of pure QGP state.

Figures 15 and 16 show the phase structure of strongly interacting matter for π^- mesons and protons produced from π^-C interaction.

Depending on the temperature T and the variable n_k (or t), the strongly interacting matter may occur in three distinct phases: the hadronic phase, the thermodynamical equilibrium, and pure QGP.

The I region covered by open circles in which the temperature T increased for π^- mesons (Fig. 15) may be connected with the thermalization of the strongly

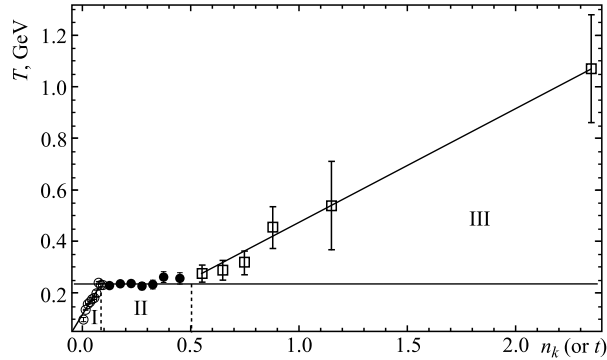


Fig. 15. The phase diagram of π^- mesons produced from π^-C interaction at 40 GeV/c

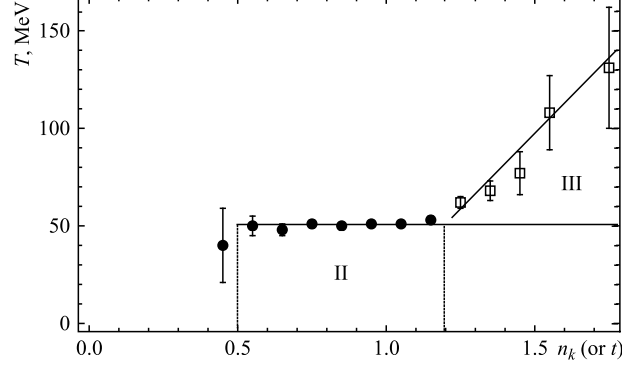


Fig. 16. The phase diagram of protons produced from $\pi^- C$ interaction at 40 GeV/c

interacting objects. In this region with the square of the three angles the strongly interacting matter is in the hadronic phase.

In the II regions covered by black circles (Figs. 15 and 16) (nearly quadratic squares), the strongly interacting matter is in the thermodynamical equilibrium phase.

In the III regions covered by open quadratics and with the square of the three angles the strongly interacting matter is in the pure QGP phase.

9. CONCLUSION

- The analysis carried out in this paper gives us the possibility to speak about the possible appearance of the phase transition of nuclear matter.
- To study the phase transition processes in hA and AA interactions at high energies, the variable n_k (or t) which is used instead of the density of nuclear matter ρ is a more appropriate variable.
- The strong changing of the characters of the above-mentioned dependences may be an indication of the different mechanism of particle production in these regions. If so, the first region with increasing T until $n_k \leq 0.1$ may correspond to the thermalization of the interacting objects (here the strongly interacting matter is in the hadronic phase), the second region with $0.1 < n_k \leq 0.5$ for π^- -mesons and with $0.4 < n_k < 1.2$ for protons may be an indication of the equilibrium state formation (hadron+QGP state), and the third region with $n_k \geq 0.5$ for mesons and $n_k \geq 1.2$ for protons can be connected with the production of pure QGP state.
- Our results show that the numerical characteristics (the temperatures in thermodynamical equilibrium and in the pure QGP state) of phase-transition processes for protons and pions are different.

Acknowledgments. We would like to express our thanks to prof. Kh. Namsrai, Prof. G. Ganbold, Prof. A. S. Sorin, Prof. A. V. Efremov and Prof. O. V. Teryaev for their valuable discussions and remarks.

REFERENCES

1. *Baldin A. M.* // Particles and Nuclei. 1977. V. 8. P. 429.
2. *Collins J. C., Perry M. J.* // Phys. Rev. Lett. 1975. V. 34. P. 1353.
3. *Polyakov A. M.* // Phys. Lett. B. 1975. V. 59. P. 82.
4. *Polyakov A. M.* // Phys. Lett. B. 1978. V. 72. P. 477.
5. *Gavani R. V., Sats H.* // Phys. Lett. B. 1984. V. 145. P. 248.
6. *Baatar Ts. et al.* JINR, P1-89424. Dubna, 1989.
7. *Baatar Ts. et al.* // J. Nucl. Phys. 1990. V. 52. P. 3(9),
8. *Balea O. et al.* // Phys. Lett. B. 1972. V. 39. P. 571.
9. *Abdurahmanov A. J. et al.* JINR, P1-6937. Dubna, 1973.
10. *Angelov N. et al.* JINR, P1-9209. Dubna, 1975.
11. *Hagedorn R.* // Nouvo Cim. Suppl. 1965. V. 3. P. 147.
12. *Rischke Dirk H.* arXiv:nucl-th/0305030v2.

Received on February 8, 2012.

Редактор *Э. В. Ивашкевич*

Подписано в печать 09.06.2012.

Формат 60 × 90/16. Бумага офсетная. Печать офсетная.

Усл. печ. л. 1,5. Уч.-изд. л. 2,06. Тираж 340 экз. Заказ № 57670.

Издательский отдел Объединенного института ядерных исследований
141980, г. Дубна, Московская обл., ул. Жолио-Кюри, 6.

E-mail: publish@jinr.ru

www.jinr.ru/publish/